



**HAL**  
open science

# Getting rid of critical raw materials in hard magnets: is it feasible?

Frédéric Mazaleyrat

► **To cite this version:**

Frédéric Mazaleyrat. Getting rid of critical raw materials in hard magnets: is it feasible?. IEEE Transactions on Magnetics, 2022, 58 (2), pp.2101110. 10.1109/TMAG.2021.3115031 . hal-03647198

**HAL Id: hal-03647198**

**<https://hal.science/hal-03647198>**

Submitted on 20 Apr 2022

**HAL** is a multi-disciplinary open access archive for the deposit and dissemination of scientific research documents, whether they are published or not. The documents may come from teaching and research institutions in France or abroad, or from public or private research centers.

L'archive ouverte pluridisciplinaire **HAL**, est destinée au dépôt et à la diffusion de documents scientifiques de niveau recherche, publiés ou non, émanant des établissements d'enseignement et de recherche français ou étrangers, des laboratoires publics ou privés.

# Getting rid of critical raw materials in hard magnets: is it feasible?

Frédéric Mazaleyrat <sup>1</sup>, *Member, IEEE*

<sup>1</sup> SATIE CNRS, Ecole normale supérieure Paris-Saclay, Université Paris-Saclay, Gif-sur-Yvette, France

Hard Magnets are key components in the evolution of transportation technologies and renewable energies. In particular in automobile industry, the anticipated switch to full electric drive in the next 30 years will create a strong demand for magnets. Unfortunately, present high performance hard magnets uses critical elements, either rare-earth or cobalt, so we can foresee a big stress on the market. In this paper, we will review all existing hard magnets having functional properties adapted to automobile electric drives, the evolution of present material to reduce the critical elements content or to get rid of them. Finally a functional cost criteria will be set and discussed.

**Index Terms**—Hard magnets, Rare-earth magnets, rare-earth free magnets, Hexaferrite, Alnico.

## I. INTRODUCTION

**C**RITICAL raw materials are key issues in many applications in the field of energy and transportations since their stock market price is highly unstable due to geopolitical reasons and increase of the demand. The problem is that all efficient hard magnets needs critical raw materials, either cobalt, platinum, rare-earth (RE) in a small or large extend (see Fig.1).

Everybody knows that the problem with Pt is its low abundance in earth-crust and relatively high demand in jewelry, for catalysis and magnetic recording, but its price is quite stable around 35 000 \$/kg. In contrast, cobalt market is volatile. It oscillates between 20 and 100 \$/kg depending mainly on the political situation in Democratic Republic of Congo, (because RDC produces 60%, i.e. 90 kt in 2018). Fig.2 illustrates the cost of Co for the last 20 years together with the political events in Congo, a clear correlation is seen: political unrest yields Co price increase whereas stability leads to a decrease. Two exception to this rule are observed, one in 2007 because of the speculation crisis mainly linked with Chinese demand and today due to the demand for automobile batteries.

The situation with RE is more complicated, one can classify RE into 2 categories: heavy RE (Gd<sup>64</sup> to Lu<sup>71</sup>), light RE (La<sup>57</sup> to Eu<sup>63</sup>). Heavy RE are scarce and usually expensive, e.g. Dy oxide price was around 125\$/kg in 2009, grew to 2300\$ during summer 2011 and then stabilized between 150 and 300\$. Light RE are more abundant, especially La<sup>57</sup>, Ce<sup>58</sup> (and Y<sup>39</sup> which chemically behaves as RE) and consequently cheaper. RE market is controlled by China where 70% of RE ore is produced though having 30% only of reserves.

So the question is why this critical materials are necessary and in which extend we can get rid of them?

The answer to this question is not straightforward because many factors have to be taken into account : price of raw elements, volatility of their market, processing cost, added value, application class and life cycle.

More than the price itself, volatility can affect the profit if the cost of raw material changes appreciably between design and production stages of a product. The processing cost may be involved if substituting an expensive element or material by

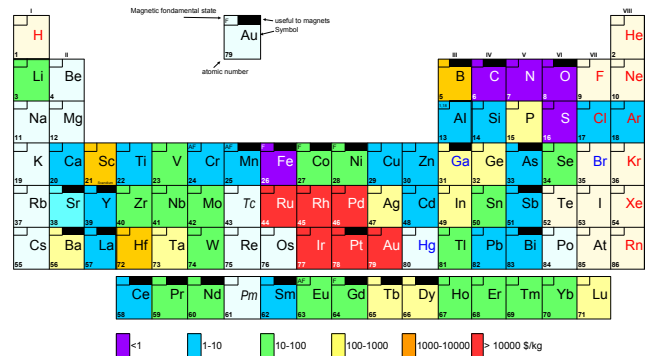


Fig. 1. The cost periodic table adapted and updated in 2020 from J.M.D. Coey [1] (note that market price of RE are given for oxides, here they have been converted to equivalent kg of pure metal)

a cheaper one is counterbalanced by an increase in processing cost. In contrast, added value can compensate the price of raw elements if it stands only for a tiny part of the total cost. For example, a luxury watch can use a 0.1g PtCo magnet because its cost would be negligible compared to advertising, total cost of precious metals or stones, trade mark, etc.

The class of application is a key parameter : the 3 main classes are aeronautics, energy production and automobile. In aeronautics, price doesn't matter compared to weight (or safety), so any element can be used if, for a given energy,

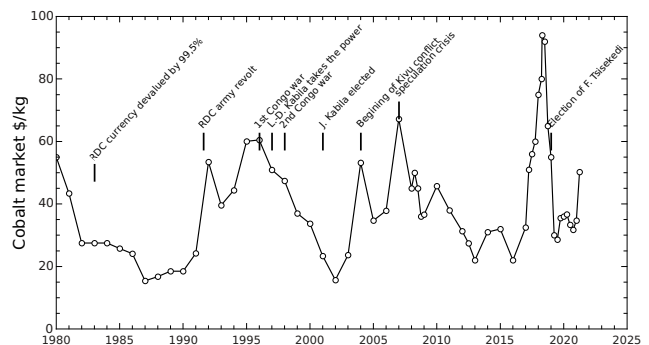


Fig. 2. The volatility of cobalt market correlated with political events and economics

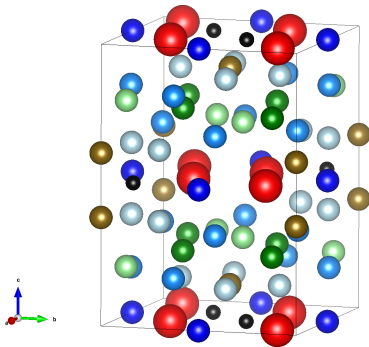


Fig. 3. Crystallographic structure of NdFeB. 8 unit formula are represented. Red Nd; black B; other colors different sites of Fe

the magnet is lighter. For energy production, e.g. in a wind turbine, the price of magnet is easily balanced by the cost of Joules losses saved over 30 years compared to a DC excitation. By opposition, a car runs typically 1000h in 3 years, so the situation is reversed compared to the wind turbine.

At last, life cycle is an important issue, magnets can be either milled and reprocessed – to the price of downgrading – or recycled from the first step of synthesis. In the latter case, separation of RE elements would be necessary and this process is costly.

In this paper we will presents the different families of hard magnets and their recent progress and we will try to find a comparison criteria to help the selection of a hard magnet.

## II. REPM

### A. Origin of the high magnetocrystalline anisotropy of REPM

The magnetocrystalline anisotropy of REPM is related to their electronic structure  $[Kr]5s^24d^{10}5p^64f^x6s^2$ . The magnetic moment is given by the  $x$  core electrons of the 4f band, so the 5p band acts as an electrostatic shield that screens 4f electrons from neighbors interactions. The consequence is a strong orbital moment, whereas transition metals (TM) one is quenched. This orbital moment is strongly coupled to both the crystal network and spin, so the atomic moment is strongly linked to the crystal. RE are usually paramagnetic at room temperature due to the low RE-RE interactions. In RE-TM intermetallic alloys, the TM conduction electrons exchange with RE 4f and, as TM-TM interactions are strong, magnetic order in intermetallic alloys occurs at room temperature and higher. Light RE elements (La to Sm) have a less than half-filled 4f band (so opposite orbital and spin moment) and ferromagnetic interactions with TM, whereas heavy RE elements (Eu to Yb) have a more than half-filled 4f band (so parallel orbital and spin moment) and antiferromagnetic interactions with TM in most compounds [2], [3]. Consequently, hard magnets should be composed mainly with light RE elements even if a heavy one can help to improve properties.

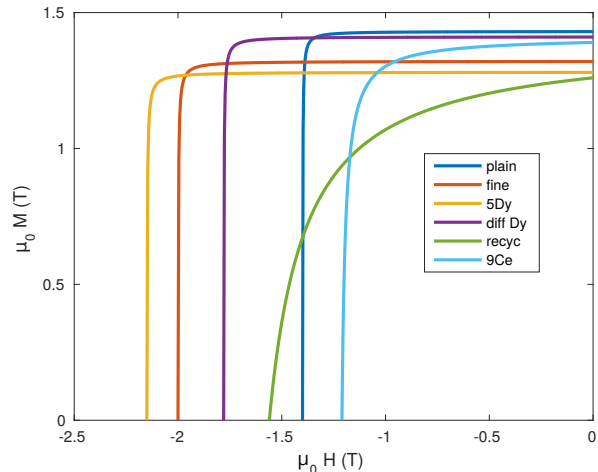


Fig. 4. Hysteresis loops of plain Nd-Fe-B (grain size  $\approx 3\mu\text{m}$ ) and fine grain ( $1\mu\text{m}$ ) [6], 5 wt.% Dy substitution [7], Dy diffusion [8], recycled [9], 9 wt.% Ce substitution [6]

### B. Iron neodymium magnets

#### 1) Non substituted Nd-Fe-B

Currently,  $\text{Nd}_2\text{Fe}_{14}\text{B}$ , aka Neomax, is the high performance magnet having the highest energy product and almost ideal hard magnetic properties [4]. It has a structure called 2-14-1,  $\text{R}_2\text{M}_{14}\text{M}'$ , of the tetragonal type (Fig.3) [5]. These magnets are mainly composed of iron which is inexpensive, abundant, with a strong magnetization. The anisotropy constant of these magnets is about  $K_1 = 5\text{MJm}^{-3}$ . The Nd is coupled ferromagnetically with Fe and the addition of interstitial B stabilizes the structure. Neomax is mainly produced in the form anisotropic sintered magnets, more rarely anisotropic bound in an organic matrix. In its original composition, it is characterized by a remanence  $B_R = 1.1\text{ T}$ , an intrinsic coercive field  $H_C^J = 1,1\text{ MA/m}$  ( $\mu_0 H_C^J = 1.4\text{ T}$ ) and therefore a extrinsic coercive  $H_C^B = 875\text{ kA/m}$  (1.1 T). Its main flaw is having a Curie point of only  $315^\circ\text{C}$  (588 K) which limits its use to  $120^\circ\text{C}$ , a clearly too low temperature in automotive applications, especially because at this temperature the coercive field is reduced to less than 0.5 T and the product energy goes from 400 to  $200\text{ kJm}^{-3}$ . Remanence is relatively unaffected but the coercive field is drastically declining. It then becomes more sensitive to demagnetization, so the slope of its load line must not be below 4. Its temperature resistance can be improved by the production process by reducing the grain size and using uniaxial compaction rather than isostatic which slightly favors density and therefore remanence.

#### 2) Heavy RE substituted Nd-Fe-B

For the uses considered here, the  $\text{Nd}_2\text{Fe}_{14}\text{B}$  magnets can be used if Nd partly is substituted for heavy RE, dysprosium (Dy) an eventually terbium (Tb). Their operating temperature can then go up to  $240^\circ\text{C}$ . The problem is that the price of these heavy RE is 10 times higher than that of the Nd which is itself already 10 times higher than it was at the origin of its use for magnets ( $>4000\text{ kg}^{-1}$ ). The most common composition contains about 1/5 of Dy, that is to say a composition close to  $\text{Nd}_{1.6}\text{Dy}_{0.4}\text{Fe}_{14}\text{B}$ . To give an order of magnitude, typically a

1 MW synchronous wind turbine contains 600 kg of magnets of this type, from which 24 kg of Dy and 110 kg of Nd.

Very recently, a new process has been developed in which the Dy is introduced by diffusion into an already sintered magnet[8]. In this way, the Dy diffuses essentially in the grain boundaries, which makes possible to increase the coercive field very significantly (nearly 40%) and to reduce the Dy rate by around 4 wt.%. As the Dy does not diffuse more than 5 mm inside the magnet, this process is limited to 10 mm thick magnets.

### 3) Nd-Fe-B substituted for Ce

All rare earths are generally found in the same ore, this is explained by the fact that these elements have the same chemical properties. When the ore is separated from light elements, one obtains the *mischmetal*, literally from German, a mixture of metal which contains Sm, Nd, Pr ... and very predominantly cerium (Ce) which is by far the most abundant and inexpensive element in this series. The  $Ce_2Fe_{14}B$  phase is indeed ferromagnetic but much less hard than its Nd counterpart. Li et al. [10] studied the properties of  $Nd_{12-x}Ce_xFe_8B_6$  for  $0 < x < 12$ , they show that the coercive field decreases linearly with the rate of Ce passing from 1.1 T to 0.7 for  $x = 8$  and drops to 0.3 for  $x = 12$ . Remanence is affected by 30%, causing the energy product to drop by a ratio of 3.

In the context of low-cost application, the 8 % Ce alloy may be an acceptable compromise, the energy product remaining above  $120 \text{ kJm}^{-3}$ , if one can accept a significant drop in the Curie point (about 20 K).

Skokov et al; [11] have shown that substitution by Ce does not significantly reduce the intrinsic magnetic properties of the crystal, but that a so-called Laves phase is formed -  $(Ce, Nd)Fe_2$  - in the interface between grains. This phase being soft, it kills the coercivity mechanisms by nucleating Bloch walls at low field. These authors [11] obtained  $\mu_0 H_C = 1.2 \text{ T}$  with an alloy  $Nd_{12}Ce_3Fe_{79}B_6$  by rapid sintering under load but on an isotropic magnet only. Tang et al. obtained an increase in coercive field by infiltration of NdCu [12].

A cheaper alternative would be to use the *mischmetal* directly. Its composition varies according to the origin of the ore but contains Ce, La, Nd, Pr in proportions of the order of 50, 25, 15, 5 plus other RE in low concentrations. The works of Li et al. [13] for a substitution up to 100% reveal a decrease of 20% in remanence, 60% of the coercive field and of 90 K in the Curie point.

### 4) Recycled NdFeB

In principle RE elements may be issued from recycling, but the elemental separation process is complicated and expensive. A solution could be to reprocess the magnets, for example by hydrogen decrepitation of DyNdFeB [9]. After orientation and bonding the properties are worst than the original (compare recyc and 5Dy curves in Fig.4), the energy product is almost divided by 2, but still acceptable for applications.<sup>1</sup>

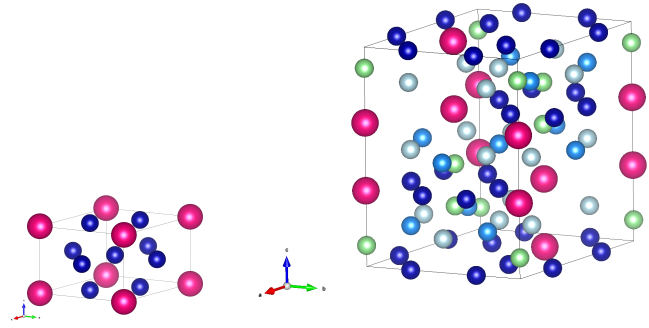


Fig. 5. Crystallographic structure of the two Sm-Co phases, left 1-5, right 2-17. Magenta Sm

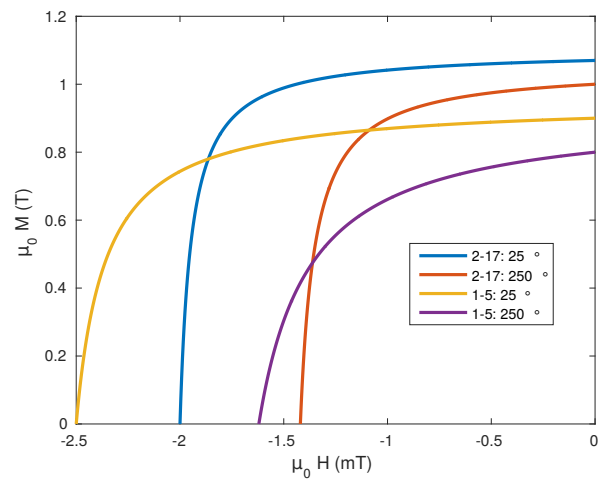


Fig. 6. Demagnetization curves of  $Sm_2Co_{17}$  and  $SmCo_5$  at room temperature and  $250^\circ C$

### C. The samarium-cobalt

Historically, Sm-Co is the first RE-based magnet [14]. It was developed in the early 1970s, but today it only represent 5% of RE-based magnets. It's relatively equivalent to Nd-Fe-B magnets substituted for Dy with a lower  $M_s$  and a higher  $H_c$ , but above all, they have better temperature stability. The abundance of Sm is 5 times lower than that of Nd, but Sm is a by-product of the production of Nd, so as long as the demand is low, the price of Sm will not increase.

Sm-Co come in two forms, 1-5 and 2-17, either  $SmCo_5$  or  $Sm_2Co_{17}$ , both of which are hexagonal although mesh 2-17 is larger. 2-17 contains less RE, but this is not a decisive cost advantage given the volatility of Co market. It was synthesized much later than the 1-5 form [15], but today it is the majority of SmCo production. Considering the elements cost, its used is restricted to high temperatures since it's the harder material existing above  $250^\circ C$ .

<sup>1</sup>Note than in the cited experiment, the authors used the full density to scale the hysteresis loop, so the remanence and energy product should be lower by the filling factor, at most 90%

TABLE I  
MAGNETICALLY HARD INTER-METALLIC PHASES.

Phase	Formula	RE (at.%)	RE (mass%)
1-5	$R_1M_5$	17	33
2-14-1	$R_2M_{14}M'$	13	26
2-17	$R_2M_{17}$	11	23
1-12	$R_1M_{12}$	8	17

#### D. The 1-12 phase

As can be seen in the TABLE I, there are mainly 4 ferromagnetic and hard inter-metallic phases. They all have a crystallographic structure of low symmetry (1 translational symmetry) unlike the Laves phases which are cubic and therefore soft. Phase 1-12 is the one containing the most ferromagnetic metal and therefore potentially the largest saturation magnetization. Logically, it is the one that contains the least rare earths, so we can see the interest there is in developing these phases.

Phase 1-12 is tetragonal, like all tetragonal magnetic phases, it is difficult to obtain. A certain number of alloys of this could be produced in the form of thin layers ( $NdFe_{12}$ ,  $SmFe_{12}$ ) with interesting properties, in particular a saturation magnetization close to 1.7 T. This process ensures the stability of the cell by epitaxy on a well-chosen substrate, but does not make it possible to produce bulk magnets. Therefore, the whole problem of phase 1-12 lies in the problem of finding the element (or the combination of elements) that will stabilize the structure.

M. Coey in his pioneering work on 1-12 [16] had proposed that one of the most promising alloys was  $SmFe_{11}Ti$ . The titanium stabilizes the structure but decreases the saturation magnetization of the compound which does not exceed 1.2 T. If the magnetic anisotropy is supposed to be high, the coercive field, on the other hand, remains almost zero. Recently, Hadjipanayis with  $Ce_{1-x}Sm_xFe_9Co_2Ti$  showed the possibility of increasing  $H_C$  to the acceptable level of 400 kA/m but at the cost of a significant drop in remanence (around 0.8 T) [17].  $NdFe_{11}Ti$  gave a strong magnetization ( $> 1.5$  T) but  $H_C < 10$  kA/m.

Substitution by zirconium has given interesting results in particular in  $Nd_{0.6}Zr_{0.4}Fe_{10}Si_2$ . Zr is a large atom which can replace part of the RE but the structure must be stabilized by the insertion of nitrogen. For the moment  $H_C < 160$  kA/m [18]. The problem is that Zr, although not critical, remains as expensive as Nd and nitrogen can quite easily come out of the mesh when the temperature rises.

### III. COBALT ALLOYS

#### A. Alnico

The Alnico, which appeared in the 1930s, have caused a revolution because their coercive field can reach 150 kA/m (compared to 20 kA/m for steels). Their composition is of type  $Al_7Ni_{14}Co_xCu_3M_yFe_{76-xy}$  where  $24 < x < 36$ , M is a refractory metal (Ti, Nb) with  $0 < y < 6$ . This formula is of course indicative, an infinity of small variations around is possible. These alloys have the characteristic of decomposing into  $\alpha Fe-Co + \alpha Ni-Al$ . A prolonged annealing around  $650^\circ C$  induces a growth of FeCo grains along their easy axis

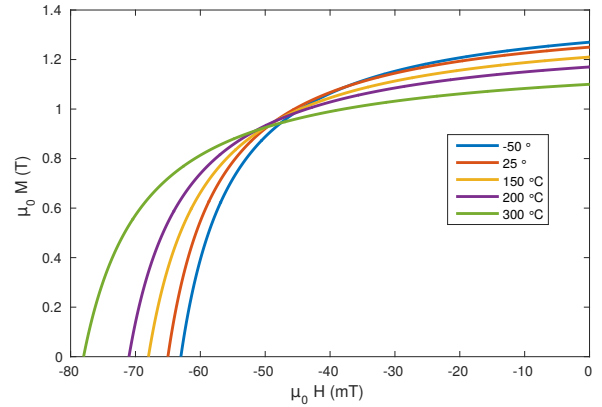


Fig. 7. Temperature dependence of Alnico 5 hysteresis loop.

with a partial diffusion of Ni towards FeCo. We then obtain a set of dispersed elongated ferromagnetic FeCo particles in a paramagnetic NiAl matrix. To get an anisotropic magnet, the alloys can be annealed under a magnetic field which orients the growth of each crystal in the direction  $\langle 100 \rangle$  closest to that of the applied field. A columnar texture can be obtained by a directed growth process consisting in slow crystallization in cold bottom crucible.

As ferromagnetic crystals are cubic, the magneto-crystalline anisotropy constant is low, also the anisotropy comes from the shape of the particles which forces magnetization along the major axis of the crystallites. In theory the reversal magnetization should only occur for a field close to  $J_S^i/\mu_0$ , where  $J_S^i$  is the intrinsic magnetization of the Fe-Co grains, i.e. above 2T. In fact, as the crystals are not thin enough, wall nucleation occurs at a field at least 10 times lower. The saturation magnetization of the magnet depends on the composition of the Fe-Co grains and the proportion of non-magnetic phase, i.e. according to the formula given above,  $0.76 - y$ . At most, if the grains have a composition close to  $Fe_2Co$ , the saturation can reach  $0.75J_S^i = 1.8$  T. For low Co rates ( $x = 24$ ) high magnetization is favored, for stronger rates ( $x = 36$ ) a high coercive field is favored.

TABLE II is showing the properties of two Alnico alloys representative of the effect of composition and process. The strongest remanence and coercivity is obtained with the directed growth process that give the most anisotropic structure with high aspect ratio of the Fe-Co crystals. The permeance coefficient ( $p$ ) is defined as the slope of the load line with a negative sign in the  $(B, \mu_0 H)$  plane (or inverse of the demagnetizing coefficient). For Alnico, it should never be lower than 10 whereas for the best ferrite and  $NdFeB$ ,  $p$  can be less than 0.5. This means that Alnico is very sensitive to demagnetization. Since 50 years Alnico did not evolve significantly, their use is now limited to high temperature, just like  $SmCo$ , except that they become harder with increasing temperature as it is shown in Fig.7.

#### B. Cobalt based semi-hard materials

Recently, the concept of hybrid magnet memory machines was proposed, in which the magnet may be magnetized

TABLE II  
PROPERTIES OF TWO ALNICO ALLOYS.

Type	composition	process	$B_R$ (T)	$H_C$ (kA/m)	$BH_{max}$ (Jm <sup>-3</sup> )	$p_{min}$
Alnico 5	Co <sub>24</sub> Ni <sub>15</sub> Al <sub>8</sub> Cu <sub>3</sub>	field cooled	1,24	48	40	30
		sintered	1,12	48	37	30
Alnico 9	Co <sub>35</sub> Ni <sub>15</sub> Al <sub>7</sub> Cu <sub>4</sub> Ti <sub>5</sub>	directed growth	1,30	56	52	20
		field cooled	1,05	112	72	10

TABLE III  
TYPICAL FEATURES OF COBALT BASED SEMI-HARD MATERIALS.

Material	Texture	$(BH)_{max}$ (kJ/m <sup>3</sup> )	$B_r$ (T)	$H_C^B$ (kA/m)
Fe <sub>35</sub> Co <sub>52</sub> V <sub>13</sub>	anisotropic	11 - 16	0.80 - 0.95	24 - 30
Fe <sub>48</sub> Co <sub>23</sub> Cr <sub>28</sub> Mo <sub>1</sub>	anisotropic	34 - 40	1.10 - 1.20	52 - 60
	isotropic	16 - 20	0.80 - 0.90	48 - 54
Fe <sub>56</sub> Co <sub>15</sub> Cr <sub>28</sub> Mo <sub>1</sub>	anisotropic	32 - 36	1.15 - 1.25	46 - 52
	isotropic	11 - 15	0.85 - 0.95	36 - 42
Fe <sub>61</sub> Co <sub>10</sub> Cr <sub>28</sub> Mo <sub>1</sub>	anisotropic	30 - 34	1.20 - 1.30	43 - 49
	isotropic	10 - 14	0.90 - 1.00	33 - 38

or demagnetize during operation [19]. These alloys have a potential for this use since they have an appreciable energy product and can be demagnetized easily.

#### 1) Fe-Co-V alloys

This semi-hard alloy is composed mainly of iron and cobalt (about 52 %) contains a high proportion of vanadium (8-14 %). The main feature of the alloy is the ductility conferred by the high rate of V (to be compared with the soft Fe-Co-V alloy, which contains only 2% of V.) They only exist in the form of sheets produced by severe cold rolling. After the annealing step, the sheet remains ductile, it can be punched and bent by the user and does not require annealing after shaping. Its Curie temperature is 700°C, but it can be used up to 500°C. The resistivity,  $70.10^{-8}\Omega m$ , is relatively high for a metal, in particular compared to Fe-Ni-Co, due to V. The energy product is comparable to that of hard ferrite, so they can be used as hard magnets but demagnetization is quite easy (see Table III).

#### 2) Fe-Co-Cr Alloy

Fe-Co-Cr is also a ductile magnet but which has the advantage of containing a high proportion of chromium, which is a very cheap element compared to Co, Ni or V. It is a magnet with magnetic properties close to those of AlNiCo but with decisive advantages such as the price of raw materials and the cost of the process. It exists in the form of strips, wires, rods, it can be stamped, cut without special tools, punched, machined, ground, etc. It exists in isotropic form and can be made anisotropic by appropriate annealing.

Compared to Fe-Co-V, this alloy is less dense  $7600\text{ kg/m}^3$ , it has comparable resistivity,  $75.10^{-8}\Omega m$ , a Curie temperature of 640°C and can be used up to about 480°C with the same restriction as Fe-Co-V.

### C. Cobalt based materials under developpement

#### 1) Cobalt nanorods

Single-domain nanoparticles can exhibit a high coercive field. Materials with a high  $K_1$  and a moderate  $M_s$ , such as

intermetallics (NdFeB, SmCo) and 3d-5d alloys (FePt, CoPt) can be mono-domain up to grain sizes of a few hundred nm and do not exhibit a superparamagnetic character if the grains are only a few nm. On the contrary, for 3d metals like cobalt, the dimensional range between the superparamagnetic state ( $\approx 10$  nm) and the division into multiple domains ( $\approx 100$  nm) quite small. This is why, in order to obtain a high coercive field with type 3d nanoparticles, it is necessary to increase the anisotropy by combining the shape anisotropy and the magnetocrystalline anisotropy. Among the various 3d ferromagnetic metals and alloys, cobalt crystallized in the hcp (hexagonal compact) structure exhibits the highest magnetocrystalline anisotropy.

The synthesis of Co nanoparticles with dimensions of the order of 1 nm in diameter and 10 nm in length has the advantage of promoting shape anisotropy. The important advantage linked to the use of these nanoparticles is their high resistance to demagnetization up to 500 K. In addition, the shape anisotropy as well as the particular shape of the particles allow easier texturing of the materials resulting from these particles. The magnetic coercive field is between 0.23 T and 0.53 T and the saturation magnetization obtained is around  $113\text{ Am}^2\text{kg}^{-1}$  ([20], [21]). However, they can't be densified without loosing their properties.

Cobalt rods with very large aspect ratio and well controlled edge shape could consolidated at low temperature (180°C, 450 MPa) with a strong orientation ( $M_R/M_S > 0.8$  [22]). Magnets made from thinner (11 nm) rods have the highest coercivity ( $\mu_0 H_C = 0.42$  T,  $\mu_0 M_R = 0.4$  T) whereas that made from 30 nm rods have better remanence ( $\mu_0 H_C = 0.28$  T,  $\mu_0 M_R = 0.82$  T) [23]. So again, the advantage of nanostructure is lost when one wants to densify the material in order to increase the magnetization.

#### 2) Cobalt carbide: Co-C

Cobalt carbides were obtained in the 1960s by decomposing an organometallic precursor. They have recently been identi-

fied as potentially hard and have been the subject of studies using the polyol route [24], the problem being that the material obtained is often composed of a mixture of  $\text{Co}_2\text{C}$  and  $\text{Co}_3\text{C}$ , the first having a rather weak magnetization. The ratio of these two phases can be controlled [25], but it is necessary to make a compromise between the coercive field of  $\text{Co}_2\text{C}$  (300 kA/m) and the magnetization of  $\text{Co}_3\text{C}$  ( $120 \text{ Am}^2/\text{kg}$ ). The best compromise leads to a saturation magnetization of  $65 \text{ Am}^2/\text{kg}$  (0.7 T) and a coercive field of 100 kA/m.

Mechanosynthesis is an alternative route but the results are similar [26]. Finally, this compound is not so hard, have a rather small magnetization and a Curie point below  $300^\circ\text{C}$ . These characteristics combined with the cost of cobalt make it an alternative with limited potential.

### 3) Cobalt-zirconium: Co-Zr

The compound  $\text{Co}_{11}\text{Zr}_2$  was identified for the first time in a recrystallized amorphous Co-Zr-B alloy [27]. Relatively hard (320 kA / m), the magnetization was quite weak due to the presence of non-magnetic phases. The alloy can also be produced by rapid quenching on a wheel in the composition  $\text{Co}_{11}\text{Zr}_2$ , but it is important to use a very fast quenching speed to directly form the rhombohedral phase and avoid the formation of the orthorhombic one [28]. The magnetization can reach  $85 \text{ Am}^2/\text{kg}$ , or in volume units the very interesting value of 0.94 T, but the coercive field is only 166 kA/m. Although it is probably possible to improve the latter value, here again the cost of cobalt is an obstacle to its development.

## IV. IRON NITROGEN

The possibly hard magnetic  $\alpha''\text{Fe}_{16}\text{N}_2$  has generated a lot of interest since its magnetization approaches 2.5 T. The  $\alpha''$  phase is very unstable and therefore very difficult to synthesize. In general this phase is found in very small proportion in nitrated iron among a multiplicity of phases: Fe,  $\text{Fe}_4\text{N}$ ,  $\text{Fe}_3\text{N}$ ,  $\text{Fe}_2\text{N}$ , of which only Fe and the  $\text{Fe}_4\text{N}$  are ferromagnetic and soft. No one has ever succeeded in obtaining a pure phase neither in thin layers nor in massive form, so the properties of  $\text{Fe}_{16}\text{N}_2$  are not well known. The non-cubic crystallographic phase of  $\alpha''$  exhibits strong magnetization due to lattice expansion produced by nitrogen insertion modifying the electronic structure of Fe (filling of the layer  $3d^1$  which has 0.2 holes in pure iron).

For 20 years, there have been numerous attempts to synthesize the compound, in the form of sheets (historically the phase was discovered steel cans in the 1940s) or of thin layers but, despite the effects of periodic announcement, very little progress has been made. At best, a partially ordered phase is obtained in layers fabricated by molecular beam epitaxy, without however obtaining a coercive field characteristic of a hard material [29]. Recently Dirba et al. made a powder of  $\text{Fe}_{16}\text{N}_2$  by reduction of hematite nanoparticles and claim to have obtained 99% of the phase. The coercive field is relatively high (more than 160 kA/m) but the magnetization is weaker than that of iron, so the result remains questionable [30].

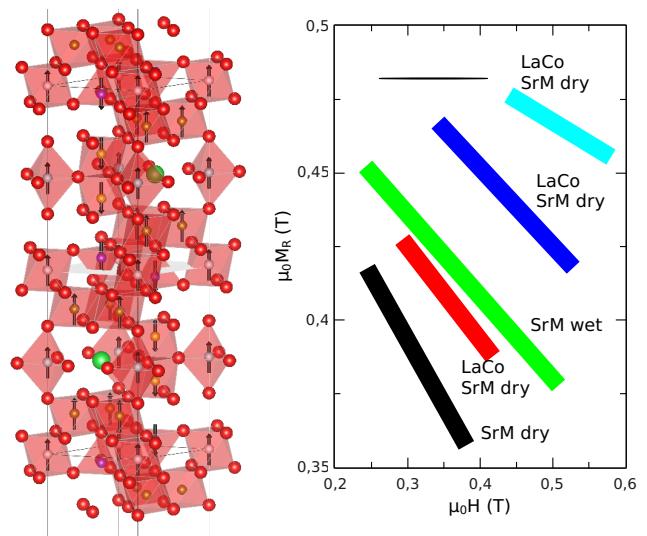


Fig. 8. Left: Crystallographic structure of magnetoplumbite. Oxygen atoms are red, Pb or Ba or Sr in green. Right: Range of magnetic characteristics achievable by different processes and composition

## V. HEXAFERRITES

### A. The Magnetoplumbite

The Magnetoplumbite, a magnetic mineral, was first discovered around 1930. Its composition and crystalline structure were determined in 1938 as hexagonal  $\text{PbFe}_{12}\text{O}_{19}$ , that we sometimes also write PbM. For the purpose of permanent magnet, Pb was first replaced by barium (BaM) and in the 70's by strontium (SrM). The magnetic characteristics of these last two compounds are very similar. The structure is a stack of  $\text{Ba}^{2+}$ ,  $\text{Fe}^{3+}$  and  $\text{O}^{2-}$  ions, the mesh being composed of two units of formula. The distribution of the  $\text{Fe}^{3+}$  ions occurs on five different crystallographic sites: a bipyramidal site ( $2b$ ), a tetrahedral site ( $4f_1$ ) and three octahedral sites ( $12k$ ,  $2a$ ,  $4f_2$ ). Each ion  $\text{Fe}^{3+}$  carries a  $5\mu_B$  magnetic spin moment parallel to c axis.

The  $\text{Fe}^{3+}$  ions are accommodated on 2 tetrahedral sites ( $2\uparrow$ ), on 1 bipyramidal site ( $1\uparrow$ ) and on 9 octahedral sites ( $7\uparrow$  and  $2\downarrow$ ), since the material is ferrimagnetic (see Fig.8 left.)

Hexaferrite hard magnets are produced either isotropic or anisotropic, the latter being the only usable for industrial applications. Though having a quite low energy product, the anisotropic SrM is a good hard magnet. Indeed, it exhibits  $\mu_0 H_C^M \approx B_R$  (so there is no risk of self demagnetization), a high curie temperature ( $455^\circ\text{C}$ ) and a positive dependence of the coercivity on temperature up to  $300^\circ\text{C}$ , so there is no risk of thermal demagnetization. Concerning the industrial production, the dry route is a cheaper process compared to wet route, but gives lower properties. For a given process, higher sintering temperature enhance the density – so the remanence – but increase the grain size, lowering the coercivity, so there is a compromise to find to optimize the properties for a given application (see Fig.8 right.)

### B. La-Co substitution

In the 60's possibility of a combined substitution with the heavy element LaCo or LaNi was shown. The trivalent

TABLE IV  
EFFECT OF THE LA-CO SUBSTITUTION ON PROPERTIES OF SRM  
HEXAFERRITE

$x$	$B_R$ (T)	$H_C^J$ (kAm <sup>1</sup> )	$H_C^J$ (T)	$(BH)_{max}$ (kJ/m <sup>3</sup> )
0	0.426	279	0.35	36
0.1	0.423	323	0.41	35
0.3	0.430	334	0.42	37
0.4	0.438	273	0.34	38

lanthanum substitutes for Ba and Co or Ni for Fe. The phase is stable but its properties did not appear to be very different from that of the normal phase, so this work was not followed up. Only 40 years later, Tenaud et al. show that the LaCo substitution in the Sr ferrite significantly increases the remanence and the coercivity [31]. An overview of the effect of the substitution rate  $x$  in  $Sr_{1-x}La_xCo_xFe_{12-x}O_{19}$  is given Table IV. Though the substitution increase  $B_R$  monotonously, at least up to  $x = 0.4$ , there is an optimum in  $H_C$  for  $x = 0.3$ , so there is a compromise to find.

The  $Co^{2+}$  ion therefore replaces the  $Fe^{3+}$  ion which allows the increase in anisotropy, and the ion  $La^{3+}$  is substituted for the ion  $Sr^{2+}$  in order to compensate the charge and because its ionic radius is close to that of strontium. Only part of the cobalt enters the M phase, which means that the semi-hard Co spinel ( $CoFe_2O_4$ ) is simultaneously produced. To avoid this phase, the Co can be only substituted at 75% of the La, the electro-neutrality is no longer satisfied but the hexaferrite lattice is stable enough to tolerate this imbalance.

Each manufacturer has his own recipe to improve the properties, using multiple substitutions, such as calcium which has slightly smaller ionic radius than La, but it's light and much less expensive.

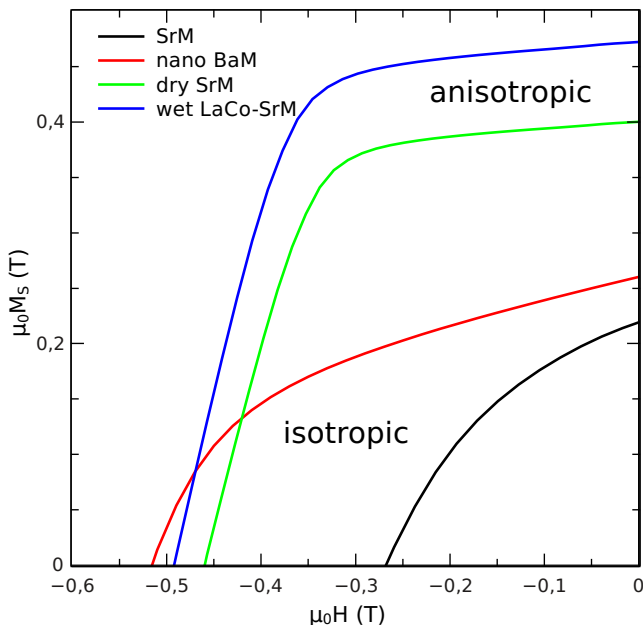


Fig. 9. Demagnetization curves of some Sr or Ba hexaferrites.

### C. Nanostructured BaM

It is well known that reducing the grain size enhances the coercive field in a spectacular way when the grain size is below the single domain limit.  $\mu_0 H_C$  as high as 0.5 T are easily achieved for particles smaller than 100 nm [32], but when sintered for densification, the coercivity drops dramatically. However, when the sol-gel process is well controlled, the particles are slightly elongated along c-axis and using spark plasma sintering at low temperature for short time, it is possible to obtain a dense anisotropic magnet with very fine grain size and high coercivity (see Fig.9 [33]). In theory, the coercivity of an isotropic material is at most  $0.48H_K$  [34], where the anisotropy field  $\mu_0 H_K = 1.7T$ . So we see that more than 60% of the theoretical value was achieved. Such fine grain material is difficult to produce in the anisotropic form, but if a technical solution is found, the coercivity could reach 1 T.

## VI. MANGANESE COMPOUNDS

### A. Heusler alloys and Mn binaries

Manganese in its pure state holds a high magnetic moment, but due to its half-filled 3d band it is fundamentally antiferromagnetic. However when alloyed with 1/2 to 3/4 of other para or diamagnetic metals, ferromagnetic order can be raised: this is often called Heusler effect, from the name of the discoverer. There are two distinct categories based on Mn: Heusler type alloys  $MnAB_2$  and MnA alloys (with A and B = Al, Bi, Cu, Ga, Ge, In, Sb, Sn, ...)

Among the equiatomic binary alloys based on Mn, two different categories must be distinguished: hexagonal structures such as MnBi and MnSb for example, and  $L1_0$  structures such as MnAl. MnBi (equi-atomic hexagonal mesh) may be a good candidate with an affordable price per kg. Bi is a scarce element, but since it is a by-product of lead with little use, it is inexpensive. However, the production of this type of magnets would create demand and increase its price. The same arguments show why compositions with Ga or Ge cannot be good candidates. Moreover, the  $M_s$  of these MnBi alloys are lower than those of Mn-Al [35] alloys.

### B. The tetragonal structure $L1_0$

Strong uniaxial anisotropy may be obtained without RE elements [36] and beyond the uniaxial crystal symmetry, the tetragonal  $L1_0$  structure is a good candidate to get hard magnetic properties as it may appear in many binary alloys. CoPt have a magnetization of  $\mu_0 M_S = 1T$ , but because they are isotropic, the remanence is about 0.6 T,  $\mu_0 H_C \approx 0.5 T$ , and  $(BH)_{max} \approx 70 kJm^{-3}$ . Their price is very high, which does not allow them to meet the technico-economical balance. FePt has even higher magnetization, but it is very difficult to produce in the bulk form, though widely used in the form of 20 nm thick layers on hard disks. FePd is also hard magnetic but it is not really an alternative since today Pd is more expensive than Pt.

Tetragonal FeNi may thus appear as a promising solution but it is found only in meteorites [37]. It takes billions of

years for these materials to achieve the thermal equilibrium necessary for the formation of this phase. Until now, nobody could synthesize tetragonal FeNi in an alloy in proportions larger than 10%.

At last, only MnAl can be produced with the tetragonal symmetry ( $\tau$ ) without critical elements. as both element are cheap, this is the only candidate with a potential industrial market.

### C. Manganese-aluminium-carbon alloys

#### D. Synthesis of Mn-Al-C

From the phase diagram of MnAl alloys [38]), we know that at low temperature, for a Mn proportion between 48.5% and 59,5%, the non-magnetic  $\gamma_2$  (trigonal phase, stable when in atomic percentage Al > Mn) and  $\beta$  (cubic phase, stable when in atomic percentage Mn > Al) phases coexist.

The ferromagnetic tetragonal phase is not an equilibrium compound, but it can be obtained after having set the hexagonal phase  $\epsilon$  by quenching, followed by annealing at a temperature of about 550°C [39], [40]). Another safer route is rapid quenching as it is very reliable to freeze the  $\epsilon$  to finally get the single  $\tau$ . Mechanical alloying is also a possible route, high energy ball milling produces an homogenous alloys with the 2 equilibrium phases, further heating at 900°C followed by annealing also yields the tetragonal phase [41].

Moreover, the  $\epsilon$  and  $\tau$  phases being metastable, it is necessary to have excess Mn in the alloy since the excess of manganese helps to form the  $\epsilon$  phase. It is also necessary to add carbon that stabilizes the  $\tau$  phase during its formation, and slows down the degradation of the materials over time. [42], [43], [44], [45], [46].

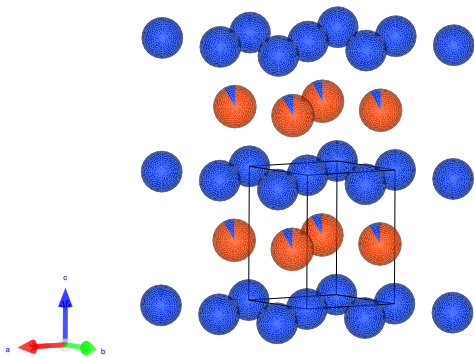


Fig. 10. Crystal structure of  $\tau$  Mn-Al. Mn is blue (site 1a), Al red (site 1d). Mn in excess to stoichiometry is represented by the blue slice in red atoms

#### E. Intrinsic magnetic properties

The intrinsic magnetic properties obtained for these alloys are about  $\mu_0 M_s = 0.65$  T,  $K_1 = 1.77$  MJm<sup>-3</sup> and of  $T_C = 370^\circ\text{C}$ . The saturation magnetization may depend on the process if some non-magnetic phase precipitates.

The phase  $\tau$  presented in the Fig.10 is composed of two crystallographic sites called 1a (0,0,0) and 1d ( $\frac{1}{2}, \frac{1}{2}, \frac{1}{2}$ ). All 1a sites are occupied by Mn atoms and 1d are occupied by

Al atoms as well as excess Mn. The atomic radius of Al is greater than that of Mn with respectively 143 pm against 137 pm so the cell is reduced along the c axis and the unit cell symmetry and size changes. From the literature ([47], [45]), we know that the moments carried by the Mn atoms of sites 1a are directed along the c axis and that these moments are ferromagnetically coupled with each other. The Slater-Bethe curve shows that a large enough distance is needed between the Mn atoms so that the coupling between the Mn atoms of the 1a sites is ferromagnetic. According to Skomski *et al.* [48], electronic structure simulation allow to determine the magnetic moments carried by the atoms of Mn and Al for equiatomic alloys. The results obtained are  $2.420 \mu_B$  for Mn and  $-0.061 \mu_B$  for Al, which shows a very weak antiferromagnetic coupling between the Mn atoms and the Al atoms. It is then predicted that the excess of Mn from the 1d sites also couples antiferromagnetically with the Mn from the 1a sites. This was experimentally shown by Tyrman *et al.* [49] by neutron diffraction. The magnetic moment of 1a site is between 2.4 and  $2.7 \mu_B \uparrow$  (depending on Mn and C content) at RT and the one of 1d is about  $3 \mu_B \downarrow$ . Thus, increasing the magnetization of the alloys means that one has to substitute the excess Mn in the 1d site.

#### F. Functional magnetic properties

For samples resulting from quenching, the coercive field is about 0.15-0.25 T,  $B_R = 0.29$  T and  $(BH)_{max} = 7$  kJm<sup>-3</sup> for an isotropic sample (see Fig.11). Usually, the product  $(BH)_{max}$  of an isotropic sample is about 4 times lower than that of an anisotropic sample. The remanence could be enhance by texturing the sample, that can be done by extrusion, but concerning the coercivity, it is not yet fully explained why it is below 0.25 T whereas the anisotropy field is 5 T. In principle, for fine grain material, one should obtain almost 1 T or even 1.5 T by comparison to the result obtained with nanostructured BaM (see sec.V-C). If the Mn-Al-C could be in the future produced in anisotropic form with a coercivity of almost 0.4 T, the energy product could reach almost 100 kJm<sup>-3</sup>.

## VII. CONCLUSION

This overview of the available materials and the state of research in the field of permanent magnets, shows that the alternatives to rare earths are for the moment extremely limited given that those available are much less efficient and not necessarily less expensive given the price of replacement elements. However, the price per kg is not the only criterion, because if we look at the performance, it is obvious that a volume of ferrite ten times greater is needed to perform the same function as an NdDyFeB.

Consequently a more judicious classification could be that of the price with equal function, i.e. for the same product  $(BH)_{max}V$  as presented TableV. We see that the conclusions are appreciably different, because magnets of average price and performance ultimately may cost more than an expensive magnet of high performance. This classification is fragile because cyclical, it can be easily affected by a change in

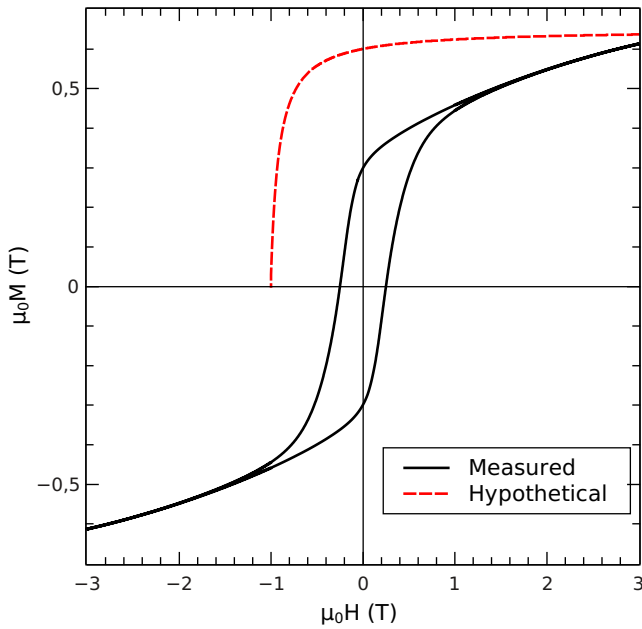


Fig. 11. Hysteresis loop of a  $Mn_{54}Al_{42}C_2$  alloy and hypothetical demagnetization curve for the same in anisotropic form.

the price of Co or Dy. This classification must also be taken with certain precautions since the machine which uses a given magnet less efficient than the reference one, will be affected in its dimensions. For a volume ratio with respect to the reference magnet  $R_{vol}$ , the overall volume of the machine will be affected by the scale factor  $R_{scl} = R_{vol}^{2/3}$ , therefore the cost of soft iron and copper will be increased by the same factor. Of course, these are only general arguments here, the optimization of the machines according to their topology and the constraints of size, temperature and weight can obviously lead to choices where the cost of the magnet is not the dominant factor.

The obvious conclusion is that, from the point of view of energy cost, the current high-performance magnets – SrLaCo ferrite, NdFeB, NdDyFeB, FeCoCr – are roughly equivalent, so that taking into account the overall cost, the most efficient and more expensive magnets may still be competitive (within the limit of minimal price variation compared to January 2021). It is clear that MnAl – thanks to an excessively low material cost, even lower than ferrites – if we manage to approach in the future an energy product close to  $100 \text{ J/m}^3$ , could upset this paradigm. However, electrical engineers will have to change drastically the design of permanent magnets machines. Indeed, in classical synchronous machines, increasing the volume of magnets means increasing the volume of both rotor and stator. In contrast, with an external stator or a disk machine, the stator volume is not affected. Another alternative would be flux switching machines that have magnet in the stator [50]. We thus see that a solution can only arise from the dialog between material scientists, electrical engineers and managers.

#### ACKNOWLEDGMENT

The author would like to thank all PhD student, post-doc or colleagues who participated directly or indirectly to this work:

TABLE V  
RANKING OF MAGNETS BY ENERGETIC COST

Material	\$/kg	\$/J	$R_{vol}$	$R_{dim}$	$R_{scl}$
MnAl*	1,00	0,06	3,33	1,49	2,23
Ferrite Sr	1,69	0,25	8,57	2,05	4,19
Ferrite SrCoLa	13,36	1,45	6,25	1,84	3,39
NdFeB	57,40	1,53	1,00	1,00	1,00
NdDyFeB	81,20	1,62	0,75	0,91	0,83
FeCoCr	14,79	1,87	5,00	1,71	2,92
Sm2Co17	69,90	2,58	1,30	1,09	1,19
Alnico 9	23,92	2,66	4,17	1,61	2,59
NdCeFeB	53,89	2,87	2,00	1,26	1,59
Alnico 5	17,04	3,40	7,50	1,96	3,83
CoPt	6 946,20	1380,60	3,75	1,55	2,41

\*Calculated

Muriel Tyrman, Andras Bartok, Alexandre Pasko, Martine LoBue, Lajos Varga (Hungarian Academy of Sciences), Ivan Guillot, Loïc Priere (ICMPE CNRS), Victor Etgens (Université Paris-Saclay), Olivier Isnard (Institut Néel), Manu Barrandiaran (University of Basque Country), sorry if I forget one...

#### REFERENCES

- [1] J. Coey, "Permanent magnets: Plugging the gap," *Scripta Materialia*, vol. 67, no. 6, pp. 524–529, 2012.
- [2] —, *Magnetism and magnetic materials*. Cambridge University Press, 2010.
- [3] R. C. O'Handley, *Modern magnetic materials*. New-York: Wiley, 2000.
- [4] M. Sagawa, S. Fujimura, N. Togawa, H. Yamamoto, and Y. Matsuura, "New material for permanent magnets on a base of nd and fe," *Journal of Applied Physics*, vol. 55, no. 6, pp. 2083–2087, 1984. [Online]. Available: <https://doi.org/10.1063/1.333572>
- [5] D. Givord, H. Li, and R. P. De La Bâthie, "Magnetic properties of Y2Fe14B and Nd2Fe14B single crystals," *Solid state communications*, vol. 51, no. 11, pp. 857–860, 1984.
- [6] B. Peng, T. Ma, Y. Zhang, J. Jin, and M. Yan, "Improved thermal stability of Nd-Ce-Fe-B sintered magnets by Y substitution," *Scripta Materialia*, vol. 131, pp. 11–14, 2017. [Online]. Available: <https://www.sciencedirect.com/science/article/pii/S1359646216306121>
- [7] K. Hono and H. Sepehri-Amin, "Prospect for hre-free high coercivity Nd-Fe-B permanent magnets," *Scripta Materialia*, vol. 151, pp. 6–13, 2018. [Online]. Available: <https://www.sciencedirect.com/science/article/pii/S1359646218301647>
- [8] K. Loewe, C. Brombacher, M. Katter, and O. Gutfleisch, "Temperature-dependent Dy diffusion processes in NdFeB permanent magnets," *Acta Materialia*, vol. 83, pp. 248–255, 2015. [Online]. Available: <https://www.sciencedirect.com/science/article/pii/S1359645414007198>
- [9] O. Gutfleisch, K. Guth, T. G. Woodcock, and L. Schultz, "Recycling used ndfeb sintered magnets via a hydrogenbased route to produce anisotropic, resin bonded magnets," *Advanced Energy Materials*, vol. 3, no. 2, pp. 151–155, 2013.
- [10] Z. Li, B. Shen, M. Zhang, F. Hu, and J. Sun, "Substitution of Ce for Nd in preparing R2Fe14B nanocrystalline magnets," *Journal of Alloys and Compounds*, vol. 628, pp. 325 – 328, 2015. [Online]. Available: <http://www.sciencedirect.com/science/article/pii/S0925838814029016>
- [11] K. Skokov and O. Gutfleisch, "Heavy rare earth free, free rare earth and rare earth free magnets - vision and reality," *Scripta Materialia*, vol. 154, pp. 289 – 294, 2018. [Online]. Available: <http://www.sciencedirect.com/science/article/pii/S1359646218300599>
- [12] X. Tang, H. Sepehri-Amin, T. Ohkubo, M. Yano, M. Ito, A. Kato, N. Sakuma, T. Shoji, T. Schrefl, and K. Hono, "Coercivity enhancement of hot-deformed Ce-Fe-B magnets by grain boundary infiltration of Nd-Cu eutectic alloy," *Acta Materialia*, vol. 144, pp. 884 – 895, 2018. [Online]. Available: <http://www.sciencedirect.com/science/article/pii/S1359645417309382>
- [13] R. Li, R. Shang, J. Xiong, D. Liu, H. Kuang, W. Zuo, T. Zhao, J. Sun, and B. Shen, "Magnetic properties of (misch metal, nd)-fe-b melt-spun magnets," *AIP Advances*, vol. 7, no. 5, p. 056207, 2017.
- [14] E. Nesbitt, R. Willens, R. Sherwood, E. Buehler, and J. Wernick, "New permanent magnet materials," *Applied Physics Letters*, vol. 12, no. 11, pp. 361–362, 1968.

- [15] H. Nagel, A. J. Perry, and A. Menth, "Hardmagnetic properties and microstructure of  $\text{sm}(\text{co},\text{cu})\text{z}$  compounds," *Journal of Applied Physics*, vol. 47, no. 6, pp. 2662–2670, 1976. [Online]. Available: <https://doi.org/10.1063/1.322987>
- [16] B.-P. Hu, H.-S. Li, J. Gavigan, and J. Coey, "Intrinsic magnetic properties of the iron-rich  $\text{thm}12$ -structure alloys  $r(\text{fe}11\text{ti})$ ;  $r = \text{y, nd, sm, gd, tb, dy, ho, er, tm}$  and  $\text{lu}$ ," *Journal of Physics: Condensed Matter*, vol. 1, no. 4, p. 755, 1989.
- [17] A. Gabay and G. Hadjipanayis, "Recent developments in  $\text{rfe}12$ -type compounds for permanent magnets," *Scripta Materialia*, vol. 154, pp. 284 – 288, 2018. [Online]. Available: <http://www.sciencedirect.com/science/article/pii/S1359646217306292>
- [18] J. Barandiaran, A. Martin-Cid, A. Schönhöbel, J. Garitaonandia, M. Gjoka, D. Niarchos, S. Makridis, A. Pasko, A. Aubert, F. Mazaleyrat *et al.*, "Nitrogenation and sintering of (Nd-Zr)  $\text{Fe}10\text{Si}2$  tetragonal compounds for permanent magnets applications," *Journal of Alloys and Compounds*, vol. 784, pp. 996–1002, 2019.
- [19] H. Yang, Z. Zhu, H. Lin, D. Wu, H. Hua, S. Fang, and Y.-k. Huang, "Novel high-performance switched flux hybrid magnet memory machines with reduced rare-earth magnets," *IEEE Transactions on Industry Applications*, vol. 52, no. 5, pp. 3901–3915, 2016.
- [20] N. Chakroune, G. Viau, C. Ricolleau, F. Fiévet-Vincent, and F. Fiévet, "Cobalt-based anisotropic particles prepared by the polyol process," *Journal of materials chemistry*, vol. 13, no. 2, pp. 312–318, 2003.
- [21] K. A. Atmane, F. Zighem, Y. Soumare, M. Ibrahim, R. Boubekri, T. Maurer, J. Margueritat, J.-Y. Piquemal, F. Ott, G. Chaboussant *et al.*, "High temperature structural and magnetic properties of cobalt nanorods," *Journal of Solid State Chemistry*, vol. 197, pp. 297–303, 2013.
- [22] E. Anagnostopoulou, B. Grindi, L.-M. Lacroix, F. Ott, I. Panagiotopoulos, and G. Viau, "Dense arrays of cobalt nanorods as rare-earth free permanent magnets," *Nanoscale*, vol. 8, no. 7, pp. 4020–4029, 2016.
- [23] S. Ener, E. Anagnostopoulou, I. Dirba, L.-M. Lacroix, F. Ott, T. Blon, J.-Y. Piquemal, K. P. Skokov, O. Gutfleisch, and G. Viau, "Consolidation of cobalt nanorods: A new route for rare-earth free nanostructured permanent magnets," *Acta Materialia*, vol. 145, pp. 290–297, 2018. [Online]. Available: <https://www.sciencedirect.com/science/article/pii/S1359645417310145>
- [24] M. Zamanpour, S. P. Bennett, L. Majidi, Y. Chen, and V. G. Harris, "Process optimization and properties of magnetically hard cobalt carbide nanoparticles via modified polyol method," *Journal of Alloys and Compounds*, vol. 625, pp. 138–143, 2015.
- [25] K. J. Carroll, Z. J. Huba, S. R. Spurgeon, M. Qian, S. N. Khanna, D. M. Hudgins, M. L. Taheri, and E. E. Carpenter, "Magnetic properties of  $\text{co}2\text{c}$  and  $\text{co}3\text{c}$  nanoparticles and their assemblies," *Applied Physics Letters*, vol. 101, no. 1, p. 012409, 2012.
- [26] Z. Turgut, M. Lucas, S. Leontsev, S. Semiatin, and J. Horwath, "Metastable  $\text{co}3\text{c}$  nanocrystalline powder produced via reactive ball milling: Synthesis and magnetic properties," *Journal of Alloys and Compounds*, vol. 676, pp. 187–192, 2016.
- [27] T. Ishikawa and K. Ohmori, "Hard magnetic phase in rapidly quenched  $\text{zr-co-b}$  alloys," *IEEE Transactions on Magnetics*, vol. 26, no. 5, pp. 1370–1372, 1990.
- [28] G.-T. Lee, K. W. Moon, K.-W. Jeon, and J. Kim, "Microstructures and magnetic properties of annealed  $\text{zr-co}$  alloys," *IEEE Transactions on Magnetics*, vol. 52, no. 7, pp. 1–3, 2016.
- [29] T. Amarouche, L.-C. Garnier, M. Marangolo, M. Eddrief, V. H. Etgens, F. Fortuna, Y. Sadaoui, M. Tamine, J. Cantin, and H. Von Bardeleben, "Influence of ion implantation parameters on the perpendicular magnetic anisotropy of  $\text{fe-n}$  thin films with stripe domains," *Journal of Applied Physics*, vol. 121, no. 24, p. 243903, 2017.
- [30] I. Dirba, C. Schwobel, L. Diop, M. Duerrschabel, L. Molina-Luna, K. Hofmann, P. Komissinskiy, H.-J. Kleebe, and O. Gutfleisch, "Synthesis, morphology, thermal stability and magnetic properties of  $\alpha''\text{-Fe}16\text{N}2$  nanoparticles obtained by hydrogen reduction of  $\gamma\text{-Fe}2\text{O}3$  and subsequent nitrogenation," *Acta Materialia*, vol. 123, pp. 214 – 222, 2017. [Online]. Available: <http://www.sciencedirect.com/science/article/pii/S1359645416308291>
- [31] P. Tenaud, A. Morel, F. Kools, J. Le Breton, and L. Lechevallier, "Recent improvement of hard ferrite permanent magnets based on  $\text{la-co}$  substitution," *Journal of alloys and compounds*, vol. 370, no. 1, pp. 331–334, 2004.
- [32] W. Zhong, W. Ding, N. Zhang, J. Hong, Q. Yan, and Y. Du, "Key step in synthesis of ultrafme  $\text{BaFe}12\text{O}19$  by sol-gel technique," *J. Magn. Mag. Mater*, vol. 168, p. 196, 1997.
- [33] Mazaleyrat, F., A. Pasko, A. Bartok, and M. LoBue, "Giant coercivity of dense nanostructured spark plasma sintered barium hexaferrite," *Journal of Applied Physics*, vol. 109, no. 7, p. 07A708, Apr. 2011.
- [34] L. Néel, "Bases d'une nouvelle théorie générale du champ coercitif," *Annales de l'université de Grenoble*, vol. 22, pp. 299–343, 1946.
- [35] J. Cui, J.-P. Choi, E. Polikarpov, M. E. Bowden, W. Xie, G. Li, Z. Nie, N. Zarkevich, M. J. Kramer, and D. Johnson, "Effect of composition and heat treatment on  $\text{mnbi}$  magnetic materials," *Acta Materialia*, vol. 79, pp. 374–381, 2014.
- [36] A. Edström, J. Chico, A. Jakobsson, A. Bergman, and J. Ruzs, "Electronic structure and magnetic properties of  $110$  binary alloys," *Physical Review B*, vol. 90, no. 1, p. 014402, 2014.
- [37] E. Poirier, F. E. Pinkerton, R. Kubic, R. K. Mishra, N. Bordeaux, A. Mubarak, L. H. Lewis, J. I. Goldstein, R. Skomski, and K. Barnak, "Intrinsic magnetic properties of  $110$   $\text{feni}$  obtained from meteorite  $\text{nwa}6259$ ," *Journal of Applied Physics*, vol. 117, no. 17, p. 17E318, 2015.
- [38] A. Shukla and A. D. Pelton, "Thermodynamic assessment of the  $\text{al-mn}$  and  $\text{mg-al-mn}$  systems," *Journal of phase equilibria and diffusion*, vol. 30, no. 1, pp. 28–39, 2009.
- [39] C. Müller, H. Stadelmaier, B. Reinsch, and G. Petzow, "Metallurgy of the magnetic  $\tau$ -phase in  $\text{mn-al}$  and  $\text{mn-al-c}$ ," *Zeitschrift fuer Metallkunde*, vol. 87, no. 7, pp. 594–597, 1996.
- [40] C. Yanar, J. Wieszorek, W. Soffa, and V. Radmilovic, "Massive transformation and the formation of the ferromagnetic  $110$  phase in manganese-aluminum-based alloys," *Metallurgical and Materials Transactions A*, vol. 33, no. 8, pp. 2413–2423, 2002.
- [41] F. Calvayrac, A. Bajorek, N. Randrianantoandro *et al.*, "Mechanical alloying and theoretical studies of  $\text{mnl}$  (c) magnets," *Journal of Magnetism and Magnetic Materials*, vol. 462, pp. 96–104, 2018.
- [42] V. Em, I. Latergaus, A. S. Remeev, and C. Lee, "Neutron diffraction study of the  $\tau$ -phase of carbon-doped  $\text{mn-al}$  alloy," *physica status solidi (a)*, vol. 159, no. 2, pp. 323–326, 1997.
- [43] J. M. Wieszorek, A. K. Kulovits, C. Yanar, and W. A. Soffa, "Grain boundary mediated displacive-diffusional formation of  $\tau$ -phase  $\text{mnl}$ ," *Metallurgical and Materials Transactions A*, vol. 42, no. 3, pp. 594–604, 2011.
- [44] A. Pasko, F. Mazaleyrat, M. LoBue, E. Fazakas, and L. Varga, "Hard magnetic properties of melt-spun  $\text{mn-al-c}$  alloys," in *EPJ Web of Conferences*, vol. 40. EDP Sciences, 2013, p. 06008.
- [45] J. Wei, Z. Song, Y. Yang, S. Liu, H. Du, J. Han, D. Zhou, C. Wang, Y. Yang, A. Franz *et al.*, " $\tau$ - $\text{mnl}$  with high coercivity and saturation magnetization," *AIP Advances*, vol. 4, no. 12, p. 127113, 2014.
- [46] A. Pasko, M. Lobue, E. Fazakas, L. Varga, and F. Mazaleyrat, "Spark plasma sintering of  $\text{mn-al-c}$  hard magnets," *Journal of Physics: Condensed Matter*, vol. 26, no. 6, p. 064203, 2014.
- [47] Q. Zeng, I. Baker, J. Cui, and Z. Yan, "Structural and magnetic properties of nanostructured  $\text{Mn-Al-C}$  magnetic materials," *Journal of magnetism and magnetic materials*, vol. 308, no. 2, pp. 214–226, 2007.
- [48] R. Skomski, P. Manchanda, P. Kumar, B. Balamurugan, A. Kashyap, and D. J. Sellmyer, "Predicting the future of permanent-magnet materials," *IEEE Transactions on Magnetics*, vol. 49, no. 7, pp. 3215–3220, 2013.
- [49] Tyrman, Muriel, A. Pasko, L. Perriere, V. Etgens, O. Isnard, and Mazaleyrat, F., "Effect of carbon addition on magnetic order in  $\text{mn-al-c}$  alloys," *IEEE Trans. Magn.*, vol. 53, p. 2101406, 2017.
- [50] E. Hoang, M. Lecrivain, and M. Gabsi, "A new structure of a switching flux synchronous polyphased machine with hybrid excitation," in *2007 European Conference on Power Electronics and Applications*, 2007, pp. 1–8.



**Frédéric Mazaleyrat** graduated in electrical engineering in 1993 and received his PhD in 1996 from Université Pierre & Marie Curie. (now Sorbonne Université). He worked first on nanocrystalline soft magnetic materials and then on the development of new soft or hard magnetics, magnetoelectrics and magnetoclorics; modeling of functional properties and applications. Hes presently a full professor at Ecole normale supérieure, Université Paris-Saclay. FM coauthored over 130 papers in peer reviewed journals, two chapters in international handbooks and two patents. He's also editor of IEEE Transaction on Magnetics and French technical encyclopedia Techniques de l'Ingenieur.